Chapter 10
Biophysical Phenomics: Evaluation of the Impact of Mycorrhization with *Piriformospora indica*

Merope Tsimilli-Michael and Reto J. Strasser

10.1 Introduction

Mycorrhizae (ecto- and endo-) are mutualistic microsymbionts of about 90 % of higher plants in natural, semi-natural and agricultural environments, with a well-documented beneficial role concerning plant growth and crop yield, especially when the soil conditions are suboptimal (degraded habitats and nutrient-deficient or polluted soil) or during stress periods (see e.g., Varma 1995, 1998; Varma and Schuepp 1996; Biro et al. 2006). They are therefore a main parameter in ecosystem functions and highly advantageous in sustainable agriculture.

Piriformospora indica, which belongs to basidiomycota, is also a root endophyte that can colonise all higher plants tested so far (including Arabidopsis and conifers), with arbuscular mycorrhizal fungi (AMF)-like characteristics and the added important advantage that, contrary to AMF that are obligate endosymbionts, it can grow axenically (it is cultivable in vitro, on agar plates or in liquid media; see e.g., Verma et al. 1998; Varma et al. 1999, 2001). Shoot and root length, biomass, basal stem, leaf area, overall size, number of inflorescences and flowers and seed production, as well as tolerance to temperature, drought and heavy metals, are all enhanced

M. Tsimilli-Michael (✉)
Ath. Phylactou 3, CY 1100 Nicosia, Cyprus
e-mail: tsimicha@spidernet.com.cy

R.J. Strasser
Weed Research Laboratory, Nanjing Agricultural University, Nanjing, China

Research Unit Environmental Science and Management, North-West University, Potchefstroom, Republic of South Africa

Laboratory of Bioenergetics, University of Geneva, Geneva, Switzerland
e-mail: Reto.Strasser@unige.ch

A. Varma et al. (eds.), *Piriformospora indica*, Soil Biology 33,
DOI 10.1007/978-3-642-33802-1_10,

in a broad range of plants, including medicinal plants, when colonised by *P. indica* (Sahay and Varma 1999; Varma et al. 2001, 2002; Rai et al. 2000, 2001, 2004; Singh and Varma 2001; Singh et al. 2000, 2002, 2003; Kumari et al. 2004; Rai and Varma 2005). Hence, *P. indica* can well be considered as a powerful new candidate symbiont for improving plant production and crop yield in sustainable agriculture, flori–horticulture and agroforestry. However, the success of any microbial inoculation in practice has to be tested for each case, since the effectiveness of symbiosis depends on complex interactions between plant, symbionts and environment.

Most of the tests focus on the estimation of root colonisation parameters (e.g., frequency, intensity) and/or the evaluation of physiological/morphological parameters (e.g., shoots and roots length and dry weight). Since mycorrhizal activity has multiple effects on the physiology and vitality of the host plant at different levels, it was reasonable to expect that it would affect, as well, the performance of the photosynthetic apparatus, which is highly sensitive to any environmental change.

Hence, we have extended our general theoretical approach of stress (Strasser 1985, 1988; Tsimilli-Michael et al. 1995, 1996) to address the establishment of symbiosis as an adaptation of plants in general, and of the photosynthetic apparatus in particular, to a changing environment (Tsimilli-Michael and Strasser 2002). Accordingly, we have applied as a testing method for recognising and, moreover evaluating, the impact of symbiosis in several cases (Tsimilli-Michael et al. 2000; Biro et al. 2006; Strasser et al. 2007; Tsimilli-Michael and Strasser 2008; Zubek et al. 2009; Jurkiewicz et al. 2010) the same experimental approach we use when addressing the impact of any other biotic or abiotic stress. This method provides a description of a biophysical phenotype in respect to the photosynthetic apparatus, which we hence termed as *Biophysical Phenomics* (Strasser and Tsimilli-Michael 2005; Strasser et al. 2007; Tsimilli-Michael and Strasser 2008). This biophysical phenotyping is a description of the behaviour/performance of photosystem (PS) II and PSI, hence an in vivo vitality analysis, in terms of different structural and functional parameters. The parameters are deduced from the JIP-test, which is an analysis of the fast chlorophyll (Chl) *a* fluorescence transient OJIP exhibited by all oxygenic photosynthetic organisms upon illumination. The method provides early diagnosis and the experimentation is simple, fast and non-invasive.

We will here review this method with representative examples of JIP-test application that reveal the beneficial impact of symbiosis with *P. indica* on the photosynthetic performance of the host plants. We will also demonstrate that the behaviour patterns of the photosynthetic machinery are similar upon colonisation either with *P. indica* or with AMF.

10.2 Biophysical Phenomics: In Vivo Analysis of Photosynthetic Behaviour/Performance

10.2.1 The Fast Chlorophyll a Fluorescence Transient OJIP

Chlorophyll (Chl) *a* fluorescence, emitted by all oxygenic photosynthetic organisms when illuminated, originates at ambient temperature basically from PSII. The analysis of the Chl *a* fluorescence kinetics and spectra has been proven to be a very useful, non-invasive tool for the investigation of stress effects on the structure and function of the photosynthetic machinery.

The fluorescence kinetics exhibited by dark-adapted photosynthetic samples upon illumination comprises a fast rise followed by a slow decline (Kautsky curve). Our method exploits the fast fluorescence rise (from 10 μs to 1 s), measured in dark-adapted leaves with a high time resolution fluorimeter (Handy-Pea fluorimeter, Plant Efficiency Analyser, Hansatech Instruments Ltd., King's Lynn Norfolk, PE 30 4NE, UK). The transients were induced by red light (peak at 650 nm) of 3,500 μmol photons m^{-2} s^{-1} intensity provided by an array of three light-emitting diodes and recorded for 1 s with 12 bit resolution. The data acquisition was every 10 μs from 10 μs to 0.3 ms, every 0.1 ms (0.3–3 ms), every 1 ms (3–30 ms), every 10 ms (30–300 ms) and every 100 ms (300 ms to 1 s).

The fast fluorescence rise is generally accepted to reflect the accumulation of the reduced form (Q_A^-) of the PSII primary electron quinone acceptor Q_A, equivalent to the closure of PSII reaction centres (RCs), which is the net result of Q_A reduction due to PSII activity and Q_A^- reoxidation due to PSI activity. When the photosynthetic sample is kept in the dark long enough to allow the full reoxidation of Q_A^-, hence the reopening of all RCs, the fluorescence intensity at the onset of illumination is denoted as F_0 (minimal fluorescence). The maximum intensity F_P at the end of the fast rise, depending on the achieved redox state of Q_A acquires its maximum possible value (denoted then as F_M) if the illumination is strong enough (usually above 500 μmol photons m^{-2} s^{-1} red light) to ensure the reduction of all Q_A (equivalently, closure of all RCs). Transients recorded with high-time-resolution fluorimeters (as e.g. the Plant Efficiency Analyzers PEA, Handy-PEA (hPEA), Pocket PEA (pPEA), Senior PEA (sPEA) and Multi-Functional PEA (mPEA), or the FluorPen and FIM instruments) provide additional and/or more accurate information concerning the processes leading to Q_A^- accumulation. It was shown that the fluorescence rise kinetics is polyphasic, exhibiting clearly, when plotted on logarithmic time scale, the steps J (at 2 ms) and I (30 ms) between the initial (F_0) and the maximum (F_P or F_M) fluorescence level (hence denoted as OJIP transient); moreover, a precise detection of F_0 (taken at 20 μs), as well of the initial slope that offers a link to the maximum rate of PSII photochemical reaction, is provided (Strasser and Govindjee 1991; Strasser et al. 1995; for reviews see Strasser et al. 2000, 2004).

10.2.2 The JIP-Test

The shape of the OJIP transient is very sensitive to stress. Strasser and co-workers have developed the JIP-test, used today world wide, which is an analysis of the OJIP fluorescence transient, by which the changes in the shape of OJIP are utilised for the detection and evaluation of the impact of several types of stress at different sites in the photosynthetic process; all three (interrelated) components of plants' vitality, namely photosynthetic activity, adaptability and stability, are hence assessed (for a review, see Strasser et al. 2004 and references therein; for the recent extension of the JIP-test that includes electron transfer through PSI, see Tsimilli-Michael and Strasser 2008; Strasser et al. 2010).

The JIP-test employs two types of data processing:

(a) Utilisation of the whole transient. Using the differences of suitably normalised transients exhibited by stressed and non-stressed plants, more bands can be detected, denoted by the series O–L–K–J–I–H–G–P, which are usually hidden among the O–J–I–P steps of the original transients (Strasser et al. 2004); the bands between the O- and P-step are labelled in alphabetic order, from slower to faster events. These phases provide a wealth of information, as they allow the recognition and, moreover, a semi-quantitative evaluation of the impact of stress on different sites of the photosynthetic machinery.

(b) Utilisation of selected original fluorescence data. On the basis of the *Energy Flux Theory in Biomembranes* (Strasser 1978, 1981), a theoretical model was developed, by which structural and functional parameters of the whole sequence of events from exciton trapping to the reduction of the PSI electron acceptor side are derived. Thus, changes in the OJIP shape are translated to changes of the structural and functional parameters.

The following original data extracted from the recorded OJIP are used (see also Table 10.1): the maximal measured fluorescence intensity, F_P, equal here to F_M since the excitation intensity is high enough to ensure the closure of all active (Q_A reducing) RCs; the fluorescence intensity at 20 μs, considered as F_0 (all RCs open); the fluorescence intensities at 50 and 300 μs ($F_{50\ \mu s}$ and $F_{300\ \mu s}$) required for the calculation of the initial slope, taken as $(dF/dt)_0 \cong (F_{300\ \mu s} - F_{50\ \mu s})/(250\ \mu s)$; the fluorescence intensities at 2 ms (J step; F_J) and at 30 ms (I-step; F_I); the complementary area (Area) above the fluorescence curve, i.e., the area between the curve, the horizontal line $F = F_M$ and the vertical lines at $t = 20$ μs and at $t = t_{F_M}$ (the time at which F_M is reached).

A schematic summary of the JIP-test concept, based on the energy fluxes and their bifurcations from PSII to the end electron acceptors of PSI, is shown in Fig. 10.1 (grey or white arrows for fluxes utilised or not for electron transfer, respectively). The figure includes definitions and equations, demonstrating also how the parameters are linked with the fluorescence signals selected from the OJIP fluorescence transient. Subscript "0" indicates that a parameter refers to the starting conditions (onset of illumination; all RCs open) of the photosynthetic sample. For more details, see Table 10.1.

Table 10.1 Glossary, definition of terms and formulae of the JIP-test parameters (see also Fig. 10.1) used for the analysis of the Chl *a* fluorescence transient OJIP emitted by dark-adapted photosynthetic samples (after Strasser et al. 2010)

Data extracted from the recorded fluorescence transient OJIP	
F_t (or, simply F)	Fluorescence at time t after onset of actinic illumination
$F_{20\ \mu s}$	First reliable recorded fluorescence at 20 μs
$F_{300\ \mu s}$	Fluorescence at 300 μs
$F_J \equiv F_{2\ ms}$	Fluorescence at the J-step (2 ms) of OJIP
$F_I \equiv F_{30\ ms}$	Fluorescence at the I-step (30 ms) of OJIP
F_P	Maximal recorded fluorescence, at the peak P of OJIP
t_{F_M}	Time (in ms) to reach the maximal possible fluorescence F_M
Area	Total complementary area between the fluorescence transient and $F = F_M$
Fluorescence parameters derived from the extracted data	
$F_0 \cong F_{20\ \mu s}$	Minimal fluorescence, when all RCs are open
F_M (=F_P)	Maximal fluorescence, when all RCs are closed ($F_M = F_P$ when the actinic light intensity is above 500 μmol photons $m^{-2}\ s^{-1}$ and provided that all RCs are active as Q_A reducing)
$F_\upsilon \equiv F_t - F_0$	Variable fluorescence at time t
$F_V \equiv F_M - F_0$	Maximal variable fluorescence
$S_m \equiv \text{Area}/(F_M - F_0) = \text{Area}/F_V$	Normalised Area
$V_t \equiv F_\upsilon/F_V \equiv (F_t - F_0)/(F_M - F_0)$	Relative variable fluorescence at time t
$M_0 \equiv [(\Delta F/\Delta t)_0]/(F_M - F_{50\ \mu s})$ $\equiv 4(F_{300\ \mu s} - F_{50\ \mu s})/(F_M - F_{50\ \mu s})$	Approximated initial slope (in ms^{-1}) of the fluorescence transient normalised on the maximal variable fluorescence F_V
Biophysical parameters derived from the fluorescence parameters	
$EC_0/RC = S_m = \text{Area}/(F_M - F_0)$	A measure of total electron carriers per RC
De-excitation rate constants of PSII antenna	
$k_N = (ABS)\ k_F\ (1/F_M)$	Nonphotochemical de-excitation rate constant (ABS: absorbed energy flux; k_F: rate constant for fluorescence emission)
$k_P = (ABS)\ k_F\ (1/F_0 - 1/F_M) = k_N\ (F_V/F_0)$	Photochemical de-excitation rate constant
Specific energy fluxes (per Q_A-reducing PSII reaction centre—RC)	
$ABS/RC = M_0\ (1/V_J)\ (1/\varphi_{Po})$	Absorption flux (of antenna Chls) per RC (also a measure of PSII apparent antenna size)
$TR_0/RC = M_0\ (1/V_J)$	Trapped energy flux (leading to Q_A reduction) per RC
$ET_0/RC = M_0\ (1/V_J)\ (1 - V_J)$	Electron transport flux (further than Q_A^-) per RC
$RE_0/RC = M_0\ (1/V_J)\ (1 - V_I)$	Electron flux reducing end electron acceptors at the PSI acceptor side, per RC

(continued)

Table 10.1 (continued)

Quantum yields and efficiencies	
$\varphi_{Pt} \equiv TR_t/ABS = [1 - (F_t/F_M)] = \Delta F_t/F_M$	Quantum yield for PSII primary photochemistry at any time t, according to the general equation of Paillotin (1976)
$\varphi_{Po} \equiv TR_0/ABS = [1 - (F_0/F_M)]$	Maximum quantum yield for PSII primary photochemistry
$\psi_{Eo} \equiv ET_0/TR_0 = (1 - V_J)$	Efficiency/probability that an electron moves further than Q_A^-
$\varphi_{Eo} \equiv ET_0/ABS = [1 - (F_0/F_M)]\,(1 - V_J)$	Quantum yield for electron transport (ET)
$\delta_{Ro} \equiv RE_0/ET_0 = (1 - V_I)/(1 - V_J)$	Efficiency/probability with which an electron from the intersystem electron carriers is transferred to reduce end electron acceptors at the PSI acceptor side (RE)
$\varphi_{Ro} \equiv RE_0/ABS = [1 - (F_0/F_M)]\,(1 - V_I)$	Quantum yield for reduction of end electron acceptors at the PSI acceptor side (RE)
$\gamma_{RC} = Chl_{RC}/Chl_{total} = RC/(ABS + RC)$	Probability that a PSII Chl molecule functions as RC
$RC/ABS = \gamma_{RC}/(1 - \gamma_{RC}) = \varphi_{Po}\,(V_J/M_0) = (ABS/RC)^{-1}$	Q_A-reducing RCs per PSII antenna Chl (reciprocal of ABS/RC)
Performance indexes (*products of terms expressing partial potentials at steps of energy bifurcations*)	
$PI_{ABS} \equiv \frac{\gamma_{RC}}{1-\gamma_{RC}} \cdot \frac{\varphi_{Po}}{1-\varphi_{Po}} \cdot \frac{\psi_o}{1-\psi_o}$	Performance index (potential) for energy conservation from photons absorbed by PSII to the reduction of intersystem electron acceptors
$PI_{total} \equiv PI_{ABS} \cdot \frac{\delta_{Ro}}{1-\delta_{Ro}}$	Performance index (potential) for energy conservation from photons absorbed by PSII to the reduction of PSI end acceptors

"Fluorescence" stands as a shortening of "fluorescence intensity"
Subscript "0" (or, "o" when written after another subscript) indicates that the parameter refers to the onset of illumination, when all RCs are assumed to be open
RC refers to the active (Q_A-reducing) PSII reaction centres

The energy fluxes are: for PSII absorption (ABS); trapping in PSII (TR_0), i.e. reduction of Pheo (pheophytin) and Q_A; electron transport (ET_0) from Q_A^- to the intersystem electron acceptors, i.e., Q_B (secondary electron quinone acceptor), PQ (plastoquinone), Cyt (cytochrome b_6/f) and PC (plastocyanin), or to any acceptor X (e.g., O_2) before PSI; reduction of end acceptors at the PSI electron acceptor side (RE_0), i.e., NADP (nicotinamide adenine dinucleotide phosphate) and Fd (ferredoxin).

The efficiencies/yields, defined as ratios of energy fluxes (and indicated by line arrows), are: the maximum quantum yield of primary photochemistry, $TR_0/ABS = \boldsymbol{\varphi}_{Po} = 1 - (F_0/F_M)$; the efficiency with which a trapped exciton can move an electron into the electron transport chain further than Q_A^-, $ET_0/TR_0 = \boldsymbol{\psi}_{Eo} = 1 - V_J$; the quantum yield of electron transport further than Q_A^-,

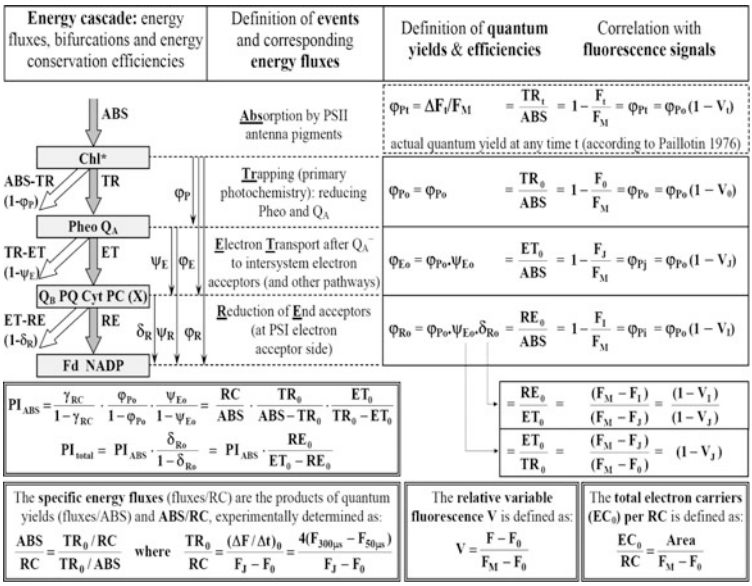

Fig. 10.1 A schematic summary of the JIP-test concept with definitions and equations, based on the energy fluxes (*wide arrows*) and their bifurcations from PSII to the end electron acceptors of PSI. Efficiencies/yields (*line arrows*) are defined as ratios of fluxes and further linked with fluorescence signals selected from the OJIP fluorescence transient. Adopted from Strasser et al. 2010. For details, see text and Table 10.1

$ET_0/ABS = \boldsymbol{\varphi}_{Eo} = \boldsymbol{\varphi}_{Po}.\ \boldsymbol{\psi}_{Eo}$; the efficiency with which an electron can move from the reduced intersystem electron carriers to the PSI end electron acceptors, $RE_0/ET_0 = \boldsymbol{\delta}_{Ro} = (1 - V_I)/(1 - V_J)$; the quantum yield for reduction of PSI end electron acceptors, $RE_0/ABS = \boldsymbol{\varphi}_{Ro} = \boldsymbol{\varphi}_{Po}.\ \boldsymbol{\psi}_{Eo}.\ \boldsymbol{\delta}_{Ro}$; the efficiency with which a trapped exciton can move an electron into the electron transport chain from Q_A^- to the PSI end electron acceptors, $RE_0/TR_0 = \boldsymbol{\psi}_{Ro} = \boldsymbol{\psi}_{Eo}.\ \boldsymbol{\delta}_{Ro}$. The definition of the relative variable fluorescence V is also given.

The derivation of the specific fluxes (fluxes per active, i.e., Q_A reducing, reaction centre-RC; arbitrary units) from the quantum yields (which are efficiencies on absorption basis; i.e., fluxes per ABS) is also depicted, as well as the derivation of the total electron carriers per reaction centre (EC_0/RC).

The figure includes also the definition of the performance indexes PI_{ABS} and PI_{total} (or PI_{tot}) as products of terms expressing energy bifurcations from PSII to the intersystem electron transport chain or to PSI end electron acceptors, respectively (where $\gamma_{RC} = Chl_{RC}/Chl_{total}$ is the fraction of PSII reaction centre Chl molecules relative to the total PSII Chl content; since $Chl_{total} = Chl_{antenna} + Chl_{RC}$, then $\gamma_{RC}/(1 - \gamma_{RC}) = Chl_{RC}/Chl_{antenna} = RC/ABS$).

10.3 Case Studies

We here chose a case study to demonstrate in detail how we apply biophysical phenomics to assess the impact of symbiosis on the photosynthetic mechanism. We started from the original fluorescence transients exhibited by dark-adapted leaves of onion plants (*Allium cepa*) that were previously obtained and partly used in an earlier publication of ours (Tsimilli-Michael and Strasser 2008), in which further details can be found. The plants were inoculated with *P. indica* or commercially available endomycorrhizae (AEGIS Endo Gel—SYTEN Company; composed of *Glomus intaradices* and *Glomus masseuse*) and grown in a greenhouse; non-inoculated plants of the same age were used as control. Figure 10.2 depicts the average Chl *a* fluorescence transient (±SD, from 20–25 replicates) for each case, expressed as F/F_0 (where F_0 is the initial fluorescence, at 20 μs), so that differences concerning the F_0 values would not interfere with the other differences. Further than demonstrating that inoculation results in bigger maximum variable fluorescence ($F_M - F_0$; normalised here on F_0), Fig. 10.2 reveals also that it causes a decrease of the heterogeneity among replicates, which is an indeed very interesting finding; moreover, heterogeneity decrease more when *P. indica* instead of AMF was used. Taken together, these two observations indicate that symbiosis has a stronger beneficial effect on the less favoured plants among the tested population.

Figure 10.3 presents the average Chl *a* fluorescence transients for the three cases (also expressed as F/F_0) to facilitate their comparison. Moreover, the figure depicts the main steps O, J, I and P and demonstrates the approximation used for calculating the initial slope. We observe that the transients exhibit differences concerning their shape. We note that the increase of the maximum variable fluorescence is equivalent to an increase of the maximum quantum yield of primary photochemistry φ_{Po} (see text; also Fig. 10.1 and Table 10.1), the parameter commonly used as the (only) criterion for comparing dark-adapted photosynthetic samples in respect to their activity.

In order to obtain a semi-quantitative evaluation of the observed differences and of other hidden differences, the three average fluorescence transients, denoted as C (non-inoculated), M (inoculated with AMF) and P (inoculated with *P. indica*), were expressed and plotted in Fig. 10.4 (left vertical axis) as kinetics of different expressions of relative variable fluorescence (see legend for details). In each of the plots (a), (b) and (c), the difference kinetics of the respective relative variable fluorescence is also presented (right vertical axis). This way of data processing permits us to get several interesting information.

The difference kinetics of $\Delta V \equiv \Delta[(F - F_0)/(F_M - F_0)]$, depicted in panel (a) together with the V kinetics, exhibit bands of negative sign in the O–I part of the OJIP transient, which indicates that processes from exciton trapping to PQ reduction (reflected in O–I; Strasser et al. 2004, 2007, 2010) are faster in inoculated

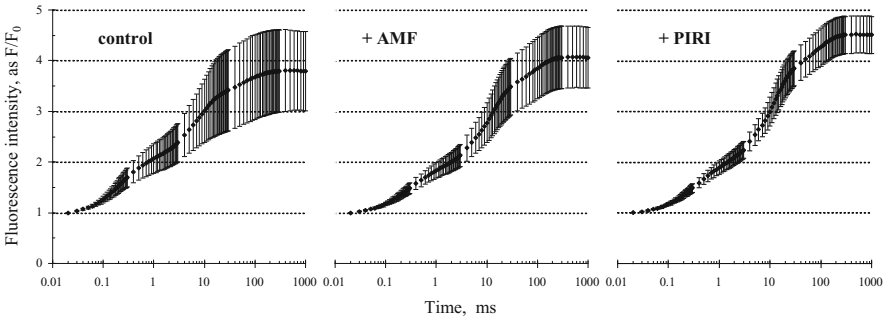

Fig. 10.2 Chl *a* fluorescence transients exhibited, upon illumination, by dark-adapted leaves of onion (*Allium cepa*) plants, which were grown without inoculation (control; *left panel*) or were inoculated with a commercial mixture of arbuscular mycorrhiza fungi (+AMF; *middle panel*) or with *P. indica* (+PIRI; *right panel*). The transients, expressed as F/F_0 (F_0 denoting the initial fluorescence intensity, taken at 20 μs, where all reaction centres (RCs) of photosystem (PS) II are considered to be open), are plotted on logarithmic time scale from 20 μs to 1 s. For each case, the average transient ± SD from 20 to 25 replicates is presented. Data were obtained from the study published by Tsimilli-Michael and Strasser (2008)

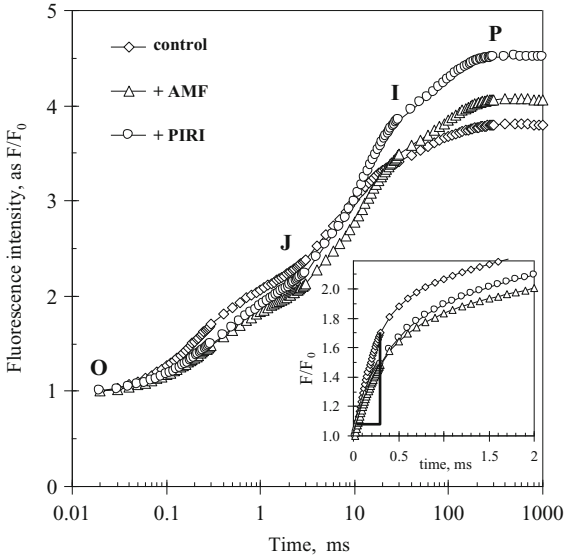

Fig. 10.3 The average Chl *a* fluorescence transients OJIP (from Fig. 10.2) are depicted, referring to onion plants that were grown without inoculation (control) or were inoculated with a mixture of arbuscular mycorrhiza fungi (+AMF) or with *P. indica* (+PIRI). The steps O (at 20 μs), J (at 2 ms), I (at 30 ms) and P (*peak*) are marked. The corresponding fluorescence intensities F_0, F_J, F_I and F_P (F_P is equal here to F_M—maximal possible intensity—due to the high excitation intensity), along with the initial slope $(dF/dt)_0$, are the selected fluorescence data used by the JIP-test for the translation of a transient to structural and functional parameters of the photosynthetic machinery (see Fig. 10.1). The approximation of the initial slope by $(\Delta F/\Delta t)_0$, taken between 50 and 300 μs, is graphically demonstrated in the *insert*, where the initial parts of the transients (up to 2 ms) are plotted on a linear time scale. For other details, see legend of Fig. 10.2

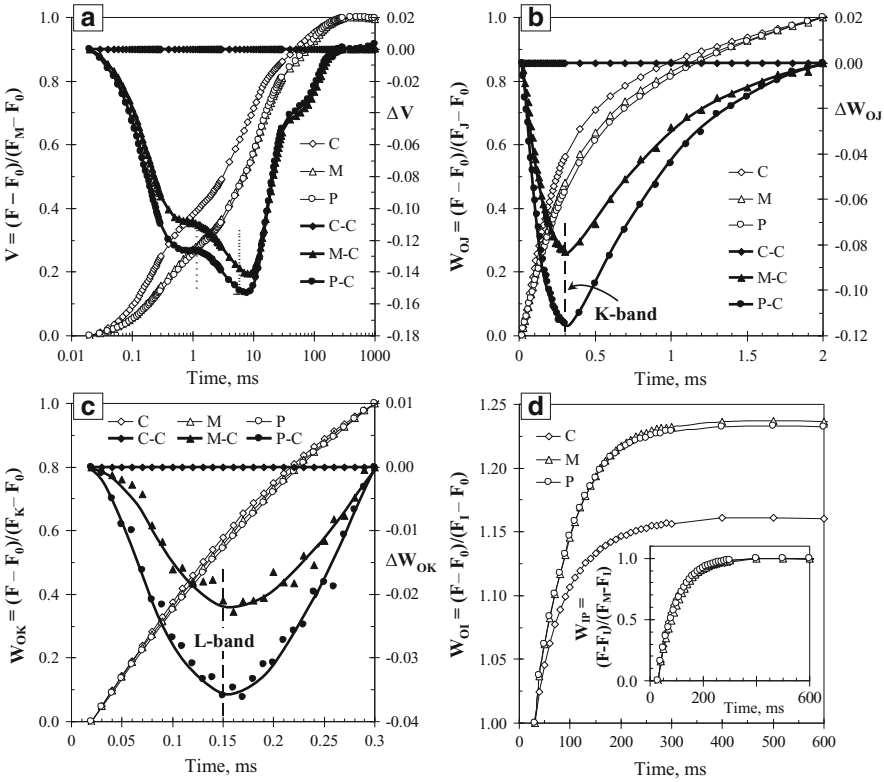

Fig. 10.4 The average Chl *a* fluorescence kinetics obtained from non-inoculated plants (C, control) and plants inoculated with arbuscular mycorrhiza fungi (M) or *P. indica* (P), and depicted as F/F_0 vs. t in Fig. 10.3, are presented (*open symbols*; *left vertical axis*) as kinetics of different expressions of relative variable fluorescence: (**a**) between F_0 and F_M, as: $V = (F - F_0)/(F_M - F_0)$; (**b**) between F_0 and F_J, as $W_{OJ} = (F - F_0)/(F_J - F_0)$; (**c**) between F_0 and $F_{300\ \mu s}$ $(= F_K)$, as $W_{OK} = (F - F_0)/(F_K - F_0)$; (**d**) between F_0 and F_I (for $F \geq F_I$), as $W_{OI} = (F - F_0)/(F_I - F_0)$ and, in the insert, between F_I and F_M (for $F \geq F_I$), as $W_{IP} = (F - F_I)/(F_M - F_I)$. In each of the plots (**a**), (**b**) and (**c**), the difference kinetics, ΔV, ΔW_{OJ} and ΔW_{OK} respectively, are also presented (*closed symbols*; *right vertical axis*). The difference kinetics were calculated by subtracting the kinetics of the control from all three kinetics and they are hence denoted as C–C, M–C and P–C. Plots (**b**) and (**c**) clearly reveal the K- and L-bands, respectively. For other details, see legend of Fig. 10.2

than in non-inoculated plants. Actually, in this time range each band is double, distinguished in a band for the O–J part (photochemical phase) and another for the J–I part (reflecting electron transfer from Q_A^- to PQ). The former indicates a higher probability of energy conservation and the latter a more efficient electron transfer to PQ. It is worth pointing out that, by this way of transient processing, the cases of AMF- and *P. indica*-inoculation cases are better resolved than in the original transients, revealing also that the effect is more pronounced when *P. indica* instead

of AMF was used. The third negative band in the I–P part of the OJIP transient will be discussed in respect to panel (d).

If we now focus on the differences concerning the O–J phase of the transients, which are revealed by the $\Delta W_{OJ} \equiv \Delta[(F - F_0)/(F_J - F_0)]$ kinetics, presented together with the W_{OJ} kinetics in panel (b), we observe bands at 300 μs, denoted in the JIP-test as K-bands. According to the interpretation of the K-band (analytically presented in Strasser et al. 2004), the negative sign of the K-bands in Fig. 10.4b indicates that the inoculated compared to the control samples have either a more active oxygen evolving system or a smaller PSII antenna size (i.e., smaller number of antenna molecules supplying excitation energy to the RC)—in other words a bigger number of active RCs per Chl. Both effects should be considered as beneficial for the photosynthetic mechanism, hence for the plant. It is worth noting that, as Fig. 10.4b reveals, the beneficial effect of *P. indica* is bigger than that of AMF.

In the plot of Fig. 10.4c, which presents the difference kinetics $\Delta W_{OK} \equiv \Delta[(F - F_0)/(F_K - F_0)]$ of the O–K phase, i.e., in the 20–300 μs time range, together with the W_{OK} kinetics, we observe bands at 150 μs, denoted in the JIP-test as L-bands. The negative sign of the L-band indicates that the extent of energetic connectivity among PSII units in the inoculated is bigger than in the non-inoculated samples, which reveals again a beneficial role of symbiosis, since energetic connectivity increases the utilisation of excitation energy and is also a factor of stability of a photosynthetic system (Strasser et al. 2004, 2007). Notably, the extent of connectivity appears to be bigger when *P. indica* instead of AMF was used.

Figure 10.4d exploits, with two different normalisations, the I–P part of the transients, which reflects processes related with the electron flow from reduced PQ (PQH_2) to PSI end electron acceptors (Schansker et al. 2005; Tsimilli-Michael and Strasser 2008; Strasser et al. 2010). With the normalisation employed for the main figure, the differences among the three cases concerning the relative amplitude of the I–P phase are depicted. We observe that this amplitude, being the same when the plants were inoculated with AMF or *P. indica*, is bigger than in non-inoculated plants. However, as revealed in the insert, where the normalisation was done between F_I and F_M, the kinetics of "filling up" the differing amplitudes are identical for all three cases. This means that symbiosis results in a bigger pool of end electron acceptors to be filled with electrons coming from PQH_2, but it does not affect the rate constants of the electron transfer pathway.

In conclusion, Fig. 10.4 demonstrates, though semi-quantitatively, that symbiosis has beneficial effects at different sites in the photosynthetic process, concerning both activity and stability, and that the beneficial effect of *P. indica* is bigger than that of AMF.

For a quantitative comparison we further analysed the fluorescence transients with the JIP-test equations and calculated a constellation of structural and functional parameters (see Fig. 10.1 and Table 10.1); each raw transient (20–25 replicates) was processed and the calculated parameters were averaged for each of the three cases of onion plants (non-inoculated or inoculated with AMF or *P. indica*). Among all the

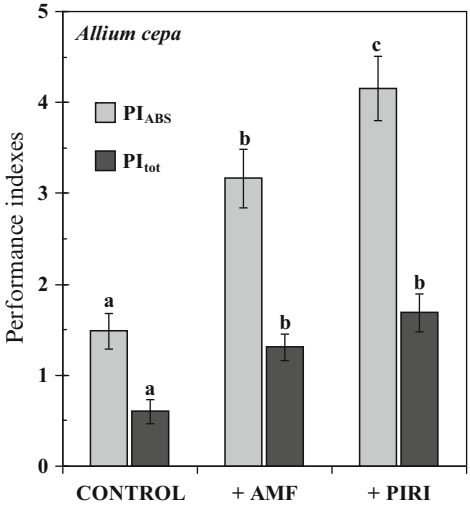

Fig. 10.5 Performance indexes PI_{ABS} and PI_{tot} (average values ± SE, from 20 to 25 replicates), calculated by analysing with the JIP-test the OJIP fluorescence transients depicted in Fig. 10.3. The plants (*Allium cepa*) were grown without inoculation (CONTROL) or were inoculated with a mixture of arbuscular mycorrhiza fungi (+AMF) or with *P. indica* (+PIRI). For each performance index, different letters above the columns indicate statistically significant differences ($P < 0.025$). For other details, see legend of Fig. 10.2

parameters determined by this analysis, the performance index PI_{tot} is the most sensitive as it evaluates the overall photosynthetic performance/behaviour; we here remind that PI_{tot} has been defined as the product of terms expressing potentials for photosynthetic performance (partial performances) at the sequential energy bifurcations from exciton up to the reduction of PSI end acceptors. Figure 10.5 presents the average PI_{tot} (± SE) for the three cases of onion plants. The other performance index, PI_{ABS}, which refers to the sequential energy bifurcations from exciton up to PQ reduction only, is also included. Figure 10.5 clearly demonstrates, in agreement with the semi-quantitative results from Fig. 10.4, that the positive effects of symbiosis are pronounced and that the benefit from inoculation with *P. indica* is bigger compared to that from inoculation with AMF.

What is more important is that the performance indexes PI_{tot} and PI_{ABS} correlate well with physiological parameters. Figure 10.6 demonstrates, as an example, the very good correlation of PI_{tot} and PI_{ABS} with the height of plants; the figure was constructed after processing fluorescence transients obtained in an earlier investigation of ours (partly used in Strasser et al. 2007), in which we applied the here presented approach for a comparative study of the beneficial role of the typical arbuscular mycorrhiza fungi *Glomus mosseae* and *Glomus caledonium* and of *P. indica* on chick pea (*Cicer arietinum* L. Chafa variety) plants exposed to cadmium (Cd) stress.

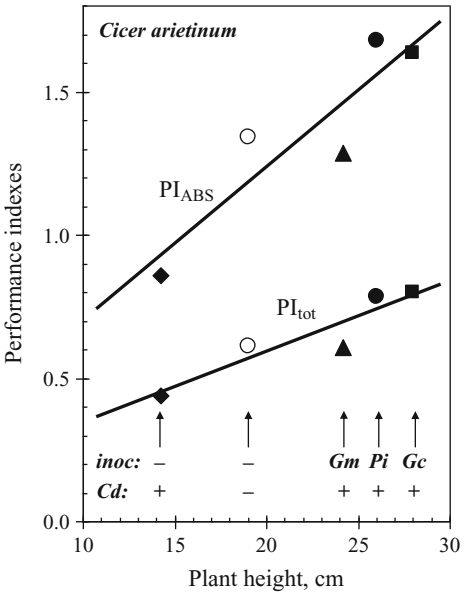

Fig. 10.6 Correlation of the performance indexes PI_{ABS} and PI_{tot} (biophysical parameters), derived by analysing with the JIP-test the OJIP fluorescence transients exhibited by dark-adapted leaves of chick pea (*Cicer arietinum* L. Chafa variety) plants, with the height of the plants (morphological parameter). The data refer to non-inoculated plants in the absence (*open circles*) or presence (*closed diamonds*) of cadmium (*Cd*) and to plants exposed to Cd stress after being inoculated with *G. mosseae* (*Gm*, *closed triangles*), *G. caledonium* (*Gc*, *closed squares*) or *P. indica* (*Pi*, *closed circles*), as indicated. Data were obtained from the study published by Strasser et al. (2007)

The performance indexes can be well used for routine screening of plants and evaluation of the overall impact of symbiosis on photosynthetic performance/behaviour. However, for a more detailed assessment of the impact at different sites the individual structural and functional parameters need to be compared. Figure 10.7 presents a collection of the so-called photosynthetic *behaviour patterns* for the analytically presented study on onion plants, the case of Cd stressed chick peas and also for four other cases where only AMF (or together with bacteria in 10.7c) was used for colonisation. Without entering in details that the reader can find in the cited references (see legend), we can clearly deduce from Fig. 10.7 that the impact of symbiosis with AMF or with *P. indica* is basically the same, both concerning the performance indexes and the individual parameters, despite differences of the extent of the impact among the six cases. It is also worth pointing out that similar behaviour patterns were found when *P. indica* or ectomycorrhiza (AEGIS Ecto Gel—SYTEN Company; composed of a spore mixture of *Rhizogon* sp., *Pisolithus* sp. and *Schleroderma* sp.) were used to colonise pine trees (*Pinus halepensis*), and that *P. indica* was found to be even more beneficial than ectomycorrhiza (Tsimilli-Michael and Strasser 2008).

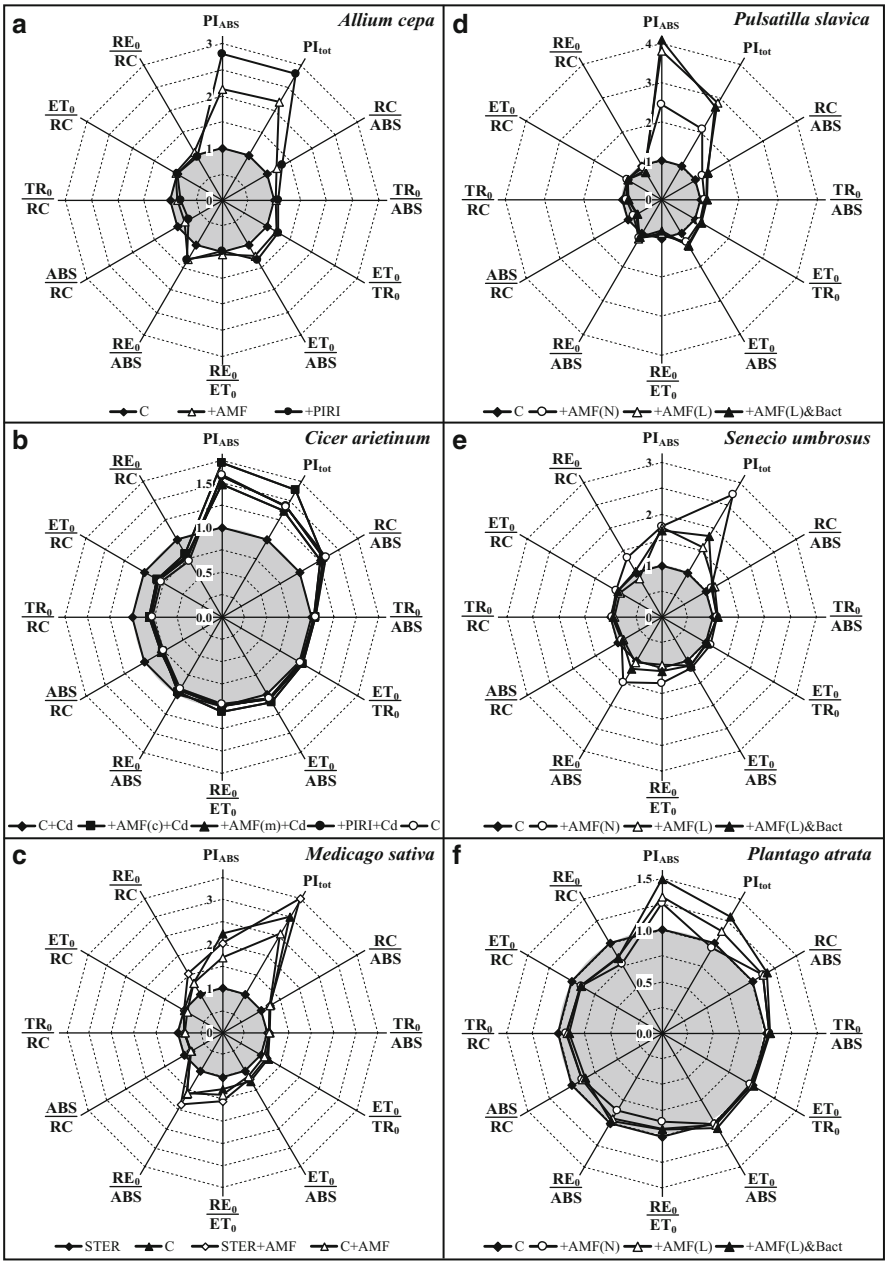

Fig. 10.7 A collection of photosynthetic behaviour patterns demonstrating the impact of symbiosis with arbuscular mycorrhiza fungi (AMF) and/or *P. indica* on six different plants grown under the same or different conditions. Each pattern comprises the same 12 structural and functional parameters and is thus presented by a dodecagon. For each plant, the parameters were derived by analysing with the JIP-test the fluorescence transients OJIP exhibited by dark-adapted leaves upon

10.4 Concluding Remarks

We have here presented a comprehensive review for the application of *Biophysical Phenomics*—a description of a biophysical phenotype in respect to the photosynthetic apparatus provided by the JIP-test—in the evaluation of the impact of mycorrhization with *P. indica* on the photosynthetic performance/behaviour, in comparison also with the impact of typical arbuscular mycorrhizal fungi. The results demonstrate that *P. indica* is equally, or even more, beneficial than AMF and that it affects in an AMF-like way the different components of the photosynthetic process. The additional take-home message of this review is that the JIP-test is a powerful tool for the in vivo and in situ recognition and evaluation of the effectiveness of symbiosis, which cannot be foreseen or taken for granted as it depends on complex interactions between plants, symbionts and environment. It should be also emphasised that the method provides early diagnosis and the experimentation is simple, fast and non-invasive. From the experimental point of view, the analytical presentation and application of our method, the JIP-test, for one

Fig. 10.7 (continued) illumination and are presented after normalisation on the corresponding values of the chosen reference case (non-inoculated plant), which is thus depicted by a regular dodecagon (values of all parameters equal to unity). Hence the deviations of the behaviour patterns of the inoculated samples from that of the reference sample demonstrate the fractional impacts of symbiosis. The photosynthetic parameters are: the quantum yields TR_0/ABS ($= \varphi_{Po}$), ET_0/ABS ($= \varphi_{Eo}$) and RE_0/ABS ($= \varphi_{Ro}$); the probabilities/efficiencies ET_0/TR_0 ($= \psi_{Eo}$) and RE_0/ET_0 ($= \delta_{Ro}$); the specific energy fluxes ABS/RC, TR_0/RC, ET_0/RC and RE_0/RC; the reaction centres per absorption (or per antenna Chl *a*), RC/ABS; the performance indexes PI_{ABS} and PI_{tot}. For the links of the parameters with fluorescence signals, see Fig. 10.1 and Table 10.1. The six panels were constructed from data obtained in previous studies of ours; for further details, see the corresponding publications. *Panel* (**a**) refers to onion (*Allium cepa*) plants grown without inoculation (C-control; reference case) or inoculated with a commercial mixture of arbuscular mycorrhiza fungi (+AMF) or *P. indica* (+PIRI); data from Tsimilli-Michael and Strasser, 2008. *Panel* (**b**) refers to chick peas (*Cicer arietinum* L. Chafa variety) that were exposed to cadmium (+Cd) stress, being either non-inoculated (C + Cd,; reference case) or inoculated with *G. caledonium* (+AMF (c) + Cd), *G. mosseae* (+AMF(m) + Cd) or *P. indica* (+PIRI + Cd); the case of non-inoculated and non-exposed to Cd stress is also depicted for comparison (C); data from Strasser et al. 2007. *Panel* (**c**) refers to alfalfa (*Medicago sativa* L.) plants grown without or with (+AMF) inoculation with *G. fasciculatum* M107, in untreated loamy chernozem soil (C), where the usual rhizosphere microflora was present, or in gamma-irradiated sterile soil (STER); the case of plants grown without inoculation in sterile soil (STER, *closed diamonds*) was used as the reference case; data from Tsimilli-Michael et al. 2000. *Panels* (**d**), (**e**) and (**f**) refer, respectively, to three endangered plant species (native in Tatra mountains, Poland), namely *Pulsatilla slavica*, *Senecio umbrosus* and *Plantago atrata*, that were either non-inoculated (C; reference case) or inoculated with native AMF isolated from their natural habitats (+AMF(N)), or a mixture of AMF strains available in the laboratory of Prof. Katarzyna Turnau in the Institute of Environmental Sciences, Jagiellonian University, Krakow, Poland (+AMF(L)) or a combination of AMF(L) with rhizobacteria (+AMF(L)&Bact); data from Zubek et al. 2009

case study (that of onion plants), can be followed easily by the reader, who can further consult, for a deeper understanding, the cited references.

References

Biro B, Köves-Péchy K, Tsimilli-Michael M, Strasser RJ (2006) Role of beneficial microsymbionts on the plant performance and plant fitness, Chap. 14. In: Mukerji KG, Manoharachary C, Singh J (eds) Microbial activity in the rhizosphere, soil biology (Varma A, Series Editor), vol 7. Springer, Berlin, pp 265–296

Jurkiewicz A, Ryszka P, Anielska T, Waligórski P, Bialońska D, Góralska K, Tsimilli-Michael M, Turnau K (2010) Optimization of culture conditions of *Arnica montana* L.: effects of mycorrhizal fungi and competing plants. Mycorrhiza 20:293–306

Kumari R, Pham GH, Prasad R, Sachdev M, Srivastava A, Yadav V, Verma PK, Sharma S, Malla R, Singh A, Maurya AK, Prakash S, Pareek A, Rexer K-H, Kost G, Garg AP, Oelmueller R, Sharma MC, Varma A (2004) *Piriformospora indica*: fungus of the millenium. In: Podila G, Varma A (eds) Basic research and applications: mycorrhizae. IK International/Kluwer Academic Press, India and New York/Holland, pp 259–295

Paillotin G (1976) Movement of excitations in the photosynthetic domains of photosystem II. J Theor Biol 58:237–252

Rai M, Varma A (2005) Arbuscular mycorrhiza-like biotechnological potential of *Piriformospora indica*, which promotes the growth of *Adhatpda vasica* Nees. Electron J Biotechnol 8:107–112

Rai M, Sahay N, Varma A (2000) In vitro growth promotion of maize and soybean by *Piriformospora indica*, an emerging endophyte. J Environ Biol 9:1–5

Rai M, Acharya D, Singh A, Varma A (2001) Positive growth responses of the medicinal plants *Spilanthus calva* and *Withania somnifera* to inoculation by *Piriformospora indica* in fields trial. Mycorrhiza 11:123–128

Rai M, Varma A, Pandey AK (2004) Antifungal potential of *Spilanthes calva* after inoculation of *Piriformospora indica*. Mycoses 47:479–481

Sahay NS, Varma A (1999) *Piriformospora indica*: a new biological hardening tool for micropropagated plants. FEMS Microbiol Lett 181:297–302

Schansker G, Tóth SZ, Strasser RJ (2005) Methylviologen and dibromothymoquinone treatments of pea leaves reveal the role of photosystem I in the Chl *a* fluorescence rise OJIP. Biochim Biophys Acta 1706:250–261

Singh A, Varma A (2001) AMF-like fungus, *Piriformospora indica*, shows promising applications. Int Symbiosis 1:1–4

Singh A, Sharma J, Rexer K-H, Varma A (2000) Plant productivity determinants beyond minerals, water and light. *Piriformospora indica*: a revolutionary plant growth promoting fungus. Curr Sci 79:101–106

Singh A, Singh A, Varma A (2002) *Piriformospora indica* - in vitro raised leguminous plants: a new dimension in establishment and phyto-promotion. Ind J Biotechnol 1:372–376

Singh A, Singh A, Kumari M, Rai MK, Varma A (2003) Biotechnology importance of *Piriformospora indica*—a novel symbiotic mycorrhiza-like fungus: an overview. Ind J Biotechnol 2:65–75

Strasser RJ (1978) The grouping model of plant photosynthesis. In: Akoyunoglou G (ed) Chloroplast development. Elsevier, Dordrecht, pp 513–524

Strasser RJ (1981) The grouping model of plant photosynthesis: heterogeneity of photosynthetic units in thylakoids. In: Akoyunoglou G (ed) Photosynthesis III. Structure and molecular organisation of the photosynthetic apparatus. Balaban International Science Services, Philadelphia, PA, pp 727–737

Strasser RJ (1985) Dissipative Strukturen als thermodynamischer Regelkreis des Photosyntheseapparates. Ber Deutsche Bot Ges Bd 98:53–72

Strasser RJ (1988) A concept for stress and its application in remote sensing. In: Lichtenthaler HK (ed) Applications of chlorophyll fluorescence. Kluwer Academic Publishers, The Netherlands, pp 333–337

Strasser RJ, Govindjee (1991) The F_0 and the O-J-I-P fluorescence rise in higher plants and algae. In: Argyroudi-Akoyunoglou JH (ed) Regulation of chloroplast biogenesis. Plenum, New York, pp 423–426

Strasser RJ, Tsimilli-Michael M (2005) State changes realizing adaptation to stress as the result of an optimized redistribution of functional microstates. In: van der Est, Bruce D (eds) Photosynthesis: fundamental aspects to global perspectives. Allen, Canada, pp 537–540

Strasser RJ, Srivastava A, Govindjee (1995) Polyphasic chlorophyll a fluorescence transient in plants and cyanobacteria. Photochem Photobiol 61:32–42

Strasser RJ, Srivastava A, Tsimilli-Michael M (2000) The fluorescence transient as a tool to characterize and screen photosynthetic samples. In: Yunus M, Pathre U, Mohanty P (eds) Probing photosynthesis: mechanism, regulation and adaptation, Chap. 25. Taylor and Francis, London, UK, pp 443–480

Strasser RJ, Tsimilli-Michael M, Srivastava A (2004) Analysis of the Chlorophyll *a* Fluorescence Transient. In: Papageorgiou GC, Govindjee (eds) Chlorophyll fluorescence: a signature of photosynthesis, advances in photosynthesis and respiration series (Govindjee—Series Editor) vol 19, chapter 12. Kluwer Academic Publishers, The Netherlands, pp 321–362

Strasser RJ, Tsimilli-Michael M, Dangre D, Rai M (2007) Biophysical phenomics reveals functional building blocks of plants systems biology: a case study for the evaluation of the impact of mycorrhization with *Piriformospora indica,* Chap. 21. In: Varma A, Oelmüller R (eds) Advanced techniques in soil microbiology, soil biology, vol 11. Springer, Berlin, Heidelberg, pp 319–342

Strasser JR, Tsimilli-Michael M, Qiang S, Goltsev V (2010) Simultaneous in vivo recording of prompt and delayed fluorescence and 820-nm reflection changes during drying and after rehydration of the resurrection plant *Haberlea rhodopensis*. Biochim Biophys Acta 1797:1313–1326

Tsimilli-Michael M, Strasser RJ (2002) Mycorrhization as a stress adaptation procedure. In: Gianinazzi S, Haselwandter K, Schüepp H, Barea JM (eds) Mycorrhiza technology in agriculture: from genes to bioproducts. Birkhauser/Verlag, Basel/Boston/Berlin, pp 199–209

Tsimilli-Michael M, Strasser RJ (2008) In vivo assessment of stress impact on plants' vitality: applications in detecting and evaluating the beneficial role of mycorrhization on host plants. In: Varma A (ed) Mycorrhiza: state of the art, genetics and molecular biology, eco-function, biotechnology, eco-physiology, structure and systematics, 3rd edn. Springer, Berlin, Heidelberg, pp 679–703

Tsimilli-Michael M, Krüger GHJ, Strasser RJ (1995) Suboptimality as driving force for adaptation: a study about the correlation of excitation light intensity and the dynamics of fluorescence emission in plants. In: Mathis P (ed) Photosynthesis: from light to biosphere, vol V. Kluwer Academic Publishers, The Netherlands, pp 981–984

Tsimilli-Michael M, Krüger GHJ, Strasser RJ (1996) About the perpetual state changes in plants approaching harmony with their environment. Archs Sci Genève 49:173–203

Tsimilli-Michael M, Eggenberg P, Biro B, Köves-Pechy K, Vörös I, Strasser RJ (2000) Synergistic and antagonistic effects of arbuscular mycorrhizal fungi and *Azospirillum* and *Rhizobium* nitrogen-fixers on the photosynthetic activity of alfalfa, probed by the chlorophyll *a* polyphasic fluorescence transient O-J-I-P. Appl Soil Ecol 15:169–182

Varma A (1995) Mycorrhizae: their application in micropropagated plantlets. Crit Rev Biotechnol 15:179–199

Varma A (1998) Mycorrhizae, the friendly fungi: what we know, what we should know and how do we know? In: Varma A (ed) Mycorrhiza manual. Springer, Germany, pp 1–24

Varma A, Schuepp H (1996) Influence of mycorrhization on the growth of micropropagated plants. In: Mukerjee KG (ed) Concepts in mycorrhizal research. Kluwer Academic Publishers, Netherlands, pp 113–132

Varma A, Verma S, Sudha SN, Bütehorn B, Franken P (1999) *Piriformospora indica*—a cultivable plant growth promoting root endophyte. Appl Environ Microbiol 65:2741–2744

Varma A, Singh A, Sudha, Sahay NS, Sharma J, Roy A, Kumari M, Rana D, Thakran S, Deka D, Bharti K, Franken P, Hurek T, Blechert O, Rexer K-H, Kost G, Hahn A, Hock B, Maier W, Walter M, Strack D, Kranner I (2001) *Piriformospora indica*: a cultivable mycorrhiza-like endosymbiotic fungus. In: Varma A, Hock B (eds) Mycota IX. Springer, Berlin, Heidelberg, New York, pp 123–150

Varma A, Singh A, Sudha, Sahay NS, Kumari M, Bharati K, Sarbhoy AK, Maier W, Walter MH, Strack D, Franken P, Singh A, Malla R, Hurek T (2002) *Piriformospora indica*: a plant stimulator and pathogen inhibitor arbuscular mycorrhiza-like fungus. In: Markandey DK, Markandey NR (eds) Microorganisms in bioremediation. Capital Book Company, New Delhi, pp 71–89

Verma S, Varma A, Rexer K-H, Hassel A, Kost G, Sarbhoy A, Bisen P, Bütehorn P, Franken P (1998) *Piriformospora indica* gen. et sp. nov., a new root-colonizing fungus. Mycologia 90:895–909

Zubek S, Turnau K, Tsimilli-Michael M, Strasser RJ (2009) Response of endangered plant species to inoculation with arbuscular mycorrhizal fungi and soil bacteria. Mycorrhiza 19:113–123